

## Transient Chaos in Dissipatively Perturbed, Near-Integrable Hamiltonian Systems

M. A. Lieberman and Kwok Yeung Tsang

*Department of Electrical Engineering and Computer Sciences and the Electronics Research Laboratory,  
University of California, Berkeley, California 94720*

(Received 13 May 1985)

When near-integrable Hamiltonian systems are perturbed by dissipation, then the stable orbits become simple attracting sinks, the Kolmogorov-Arnol'd-Moser tori are destroyed, and persistent chaotic motion disappears. We determine analytically the mean lifetime, the quasistatic distribution, and the fraction trapped into the various sinks for a dissipatively perturbed area-preserving twist map.

PACS numbers: 03.20.+i, 02.50.+s, 05.40.+j, 05.45.+b

Two-dimensional, near-integrable, measure-preserving maps are used to model conservative physical phenomena in such fields as celestial mechanics, cosmic-ray physics, accelerator theory, and plasma heating and confinement.<sup>1</sup> Conservative systems of two nonlinear coupled oscillators are also used widely as physical models. This system motion also generates such maps as the phase-space orbit repeatedly pierces a surface of section.

The phase-plane structure in near-integrable measure-preserving maps is well known.<sup>2</sup> There is persistent regular motion on some perturbed Kolmogorov-Arnol'd-Moser (KAM) orbits and on KAM "island" orbits surrounding stable fixed points of the map. Regions of persistent chaotic motion are densely interwoven with these regular regions. The measures of the regular and chaotic regions can vary widely, both within the phase plane and as a function of the system parameters.

This structure is not stable under dissipative perturbation. The stable fixed points become attracting centers (sinks), and all KAM curves are destroyed. Although transient chaotic motion generally exists, the phase point eventually enters an embedded island and is attracted to an island sink; the motion ultimately becomes periodic. The complete destruction of persistent chaos when a weak dissipation is added to a near-integrable Hamiltonian system is typical and probably generic behavior. It is clearly of interest to understand this degeneration from persistent to transient chaos.

In this Letter, we present the first analytical study of transient chaotic motion for a class of near-integrable Hamiltonian twist maps<sup>2</sup> that are perturbed by dissipation. We determine analytically such properties as the mean lifetime for chaotic motion, the quasistatic distribution for the transiently chaotic region, and the probability of trapping into the various embedded islands.

We note that above a critical dissipation strength, a new type of attractor ("strange attractor") in the phase plane can appear, on which the motion is persistent and chaotic.<sup>3-5</sup> We have considered this case

elsewhere.<sup>6,7</sup>

We illustrate the calculation procedure for transient chaos using as an example the dissipative Fermi map.<sup>6,7</sup> However, the procedure is directly applicable when dissipation is introduced into other twist maps such as the Chirikov-Taylor<sup>8,9</sup> and the separatrix maps.<sup>2,8</sup> The Fermi map describes a cosmic-ray acceleration mechanism<sup>10</sup> in which charged particles are accelerated by collisions with moving magnetic field structures. In the model, a ball bounces in one-dimensional motion between a fixed and an oscillating wall. We adapt a simplified model<sup>11</sup> in which the moving wall oscillates sinusoidally,  $x_w(t) = a \cos \omega t$ , and elastically imparts momentum to the ball according to its velocity  $\dot{x}_w$  without the wall changing its position in space. We introduce dissipation by assuming that the ball suffers a fractional loss  $\delta$  in velocity upon collision with the fixed wall. The map is then

$$\bar{u} = (1 - \delta)u_n - \sin \psi_n, \quad (1a)$$

$$\bar{\psi} = \psi_n + 2\pi M/\bar{u}, \quad (1b)$$

$$(\psi_{n+1}, u_{n+1}) = (\bar{\psi}, \bar{u}) \operatorname{sgn} \bar{u}, \quad (1c)$$

where  $u_n = v_n/2\omega a$  is the normalized ball velocity and  $\psi_n = \omega t_n$  is the phase of the oscillating wall, and  $M = l/(2\pi a)$  is the normalized distance between the two walls. The functions  $\operatorname{sgn} \bar{u} = \pm 1$  for  $\bar{u} \gtrless 0$ , and is introduced to maintain  $u_{n+1} \geq 0$  for low velocities  $u_n < (1 - \delta)^{-1}$ , as physically occurs in the exact model, while preserving the continuity of the map near  $u = 0$ . The Jacobian of the map is  $1 - \delta$ , and thus the map is area preserving for  $\delta = 0$ .

The primary fixed points of the map are found by setting  $u_{n+1} = u_n$  and  $\psi_{n+1} = \psi_n \pmod{2\pi}$  in (1). We obtain

$$(u_k, \psi_k) = (M/k, \sin^{-1}(-u_k \delta)), \quad (2)$$

where  $k$  is an integer. There are two fixed points for each  $k$ :  $\psi_k \approx 0$  or  $\psi_k \approx \pi$  for  $u_k \delta \ll 1$ .  $\psi_k \approx \pi$  is stable for  $u_k > u_s = (\pi M/2)^{1/2}$ ;  $\psi_k \approx 0$  is always unstable. For  $\delta = 0$ , invariant (KAM) island orbits sur-

round the stable fixed points. The location, stability, and bifurcations of these fixed points have been described in detail previously.<sup>2,11-14</sup>

We summarize the behavior of the motion, determined by numerical iteration, as the parameters  $M$  and  $\delta$  are varied. For  $\delta=0$ , there is no dissipation and the usual Hamiltonian chaos ensues, with intermingled areas of persistent chaotic and regular motion in the  $(u, \psi)$  phase plane. Numerical iterations for  $10 \leq M \leq 10^4$  show<sup>11-14</sup> that the phase plane divides into three characteristic regions: (1) For large velocities,  $u > u_b \approx 2u_s$ , invariant (KAM) curves span the plane in  $\psi$  and isolate the narrow layers of stochasticity near the separatrices surrounding the fixed points of the map; (2) there is an interconnected stochastic region for intermediate velocities,  $u_b > u > u_s$ , in which invariant islands near stable fixed points of the map are embedded in a stochastic sea; and (3) there is a predominantly stochastic region for small velocities,  $u < u_s$ , in which all primary fixed points are unstable. The globally stochastic motion within the connected regions (2) and (3) is isolated from region (1) by a KAM barrier at  $u_b$ , and has a constant equilibrium invariant distribution  $f_0(u, \psi)$ .<sup>15</sup>

For weak dissipation,  $0 < \delta < \delta_c$ , the numerical iterations show that the fixed points of the Hamiltonian map become attracting centers (sinks), the KAM curves no longer exist, and all persistent chaotic motion is destroyed. However, transient chaotic motion surrounds the sinks in regions (2) and (3). As an example, for  $M=30$  ( $\delta_c \approx 0.02$ ) and  $\delta=0.003$ , we find that an initial phase point chosen randomly in region (3) undergoes transient chaotic motion for a mean number of iterations  $\bar{N} \approx 13\,000$  before it enters an embedded island in region (2) and becomes trapped in an island sink. For the eleven cases studied, the decay from the transiently chaotic region is observed to be exponential at a rate  $\bar{\alpha} = \bar{N}^{-1}$ , which is tabulated as the first entry in Table I.

In Fig. 1, we plot the cumulative phase-integrated distribution

$$\bar{f}(u) = 100 \int_0^N dn \int_0^{2\pi} d\psi f(u, \psi, n),$$

for  $M=30$ ,  $\delta=0.003$ , after  $N=5 \times 10^4$  iterations, for 100 initial conditions at low velocities chosen randomly. We see evidence of attracting sinks between  $u_s$  and  $u_b$  near the primary resonances at  $k=3$  (a period-1 and a period-5 sink coexist) and at  $k=4$  (a period-1 and a period-3 sink coexist). The density leaving the stochastic region flows into these sinks, forming spikes in the figure. For all cases studied, the location and structure of these sinks correspond to the Hamiltonian ( $\delta=0$ ) structure of the stable fixed points (2) of the Fermi map. The period-3 and period-5 sinks correspond to secondary fixed points encircling the period-1 primary fixed points, as described in Ref. 1, Sect. 2.4.

TABLE I. Numerically and analytically determined decay rates  $\bar{\alpha}$  (in units of  $10^{-5}$ ), for various values of  $M$  and  $\delta$ .

$M$	$\delta$			
	0.0003	0.001	0.003	0.01
30	2.0/2.5	2.7/6.6	7.4/12.0	7.7/8.6
100	1.2/2.0	2.0/3.6	2.9/2.6	1.1/0.29
300	1.1/1.1	1.1/0.90	0.40/0.16	...

Numerical studies for various values of  $N$ ,  $M$ , and  $\delta \ll 1$  show that an exponentially decaying *quasistatic* distribution

$$f(u, \psi, n) = f_Q(u) \exp(-\bar{\alpha}n) \quad (3)$$

is formed for  $n \geq u_b^2 \approx 2\pi M$ , for values of  $u$  outside of the ‘‘sticky’’ islands.

The distribution  $f_Q$  can be found analytically by solving the appropriate Fokker-Planck equation for the map<sup>16</sup>

$$\frac{\partial f}{\partial n} = \frac{1}{2} \frac{\partial}{\partial u} \left[ D \frac{\partial f}{\partial u} \right] - \frac{\partial (Bf)}{\partial u} \approx 0, \quad (4)$$

where, to first order in  $\delta$ ,  $D$  is the diffusion coefficient for the area-preserving ( $\delta=0$ ) map, and  $B = -u\delta$  is the friction coefficient due to the dissipation.<sup>15</sup> For  $u \leq u_s$ ,  $D = \frac{1}{2}$ , the quasilinear value. However, the domain of interest includes the region  $u_s \leq u \leq u_b$ , in which the quasilinear diffusion coefficient is invalid. To obtain an estimate of  $D$  in this region, we locally expand (1) in  $u$  about a fixed point  $u_k$ , which yields

$$I_{n+1} = I_n(1 - \delta) + K \sin\theta_n - u_k \delta, \quad (5a)$$

$$\theta_{n+1} = \theta_n + I_{n+1}, \quad (5b)$$

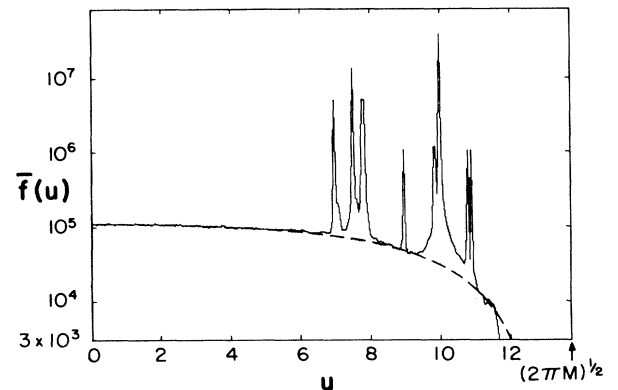


FIG. 1. Cumulative, phase-averaged distribution  $\bar{f}$  vs  $u$ , for  $M=30$ ,  $\delta=0.003$ , and  $N=5 \times 10^4$  iterations. The solid curve shows the numerical result; the dashed curve shows the quasistatic theory.

where

$$I_n = -K(u_n - u_k), \quad (6a)$$

$$\theta_n = \psi_n, \quad (6b)$$

and

$$K = 2\pi M/u_k^2 \quad (7)$$

is the stochasticity parameter. For  $\delta=0$ , (5) is the Chirikov-Taylor or "standard" map,<sup>17</sup> which has a diffusion coefficient  $\bar{D}$  that depends on  $K$ . For  $K \geq 4$ , corresponding to  $u \leq u_s$ , we have  $\bar{D} \approx K^2/2$ , the quasilinear value. For  $4 \geq K > 1$ , corresponding to  $u_s \leq u < u_b$ , one finds

$$\bar{D} \propto (K-1)^\gamma,$$

with the estimate<sup>8</sup>  $\gamma \approx 2.5$  for  $4 \geq K > 1$  obtained numerically, and the asymptotic result<sup>18,19</sup> near  $K=1$ ,  $\gamma \approx 3.01$ . However, over the entire range  $K > 1$ , a reasonable fit to the numerical data for  $\bar{D}$  is

$$\bar{D} \approx \frac{K^2}{2} \left( \frac{K-1}{K} \right)^\gamma, \quad (8)$$

with  $\gamma=2$ . Transforming from  $I$  back to  $u$ , we have  $D = \bar{D}/K^2$ , and with use of (7) and (8), we obtain, for  $u < u_b$ ,

$$D = \frac{1}{2} (1 - u^2/u_b^2)^2. \quad (9)$$

Using  $B = -u\delta$  and (9) in (4) and the condition that the net flux is zero, we obtain

$$f_Q(u) = F \exp[-2\beta u^2/(u_b^2 - u^2)], \quad (10a)$$

where

$$F = (2\pi u_b \beta)^{-1} [K_1(\beta) - K_0(\beta)]^{-1} \times \exp(-\beta), \quad (10b)$$

$\beta = u_b^2 \delta$ ,  $K_1$  and  $K_0$  are the modified Bessel functions, and

$$2\pi \int_0^{u_b} du f_Q(u) = 1.$$

This distribution, scaled to the value of  $\bar{f}$  at  $u=0$ , is plotted as the dashed line in Fig. 1. The agreement with the numerical result outside the island regions is excellent. Equally good agreement is found for all other cases listed in Table I.

We now determine the phase-space area  $\Delta A_k$  in the transiently chaotic region that is "eaten" by each primary island during one iteration. The standard map [(5) with  $\delta=0$ ] has a closed KAM barrier  $I(\theta)$  with area  $\bar{A}$  surrounding the central fixed point  $(I, \theta) = (0, \pi)$ . This barrier curve separates the outer chaotic region from the inner closed island orbits. For  $\delta > 0$ ,  $\bar{A}$  contracts by the factor  $1 - \delta$ . Thus  $\Delta \bar{A} = \bar{A} \delta$ . Transforming back to  $(u, \psi)$  variables using (6), we

obtain

$$\Delta A_k(u_k) = \bar{A} \delta / K. \quad (11)$$

$\bar{A}$  is a function of  $K = u_b^2/u_k^2$  alone that can be found analytically<sup>19,20</sup> or numerically.<sup>8</sup> A good approximation for  $1 < K < 6$  is  $\bar{A} \approx 2\pi^2 K^{-1.3}$ . For the results in Table I, we determine  $\bar{A}$  numerically by setting  $\delta=0$  in the first term on the right-hand side of (5a). The small correction in  $\bar{A}$  due to the last term  $-u_k \delta$  in (5a) was therefore included.

Chirikov and Izraelev<sup>21</sup> showed numerically that the decay rate due to a sink varies directly as  $\Delta A_k$ . For nonuniform  $f_Q$ , however, the decay rate should also be proportional to  $f_Q$  at the sink. Using (10) and (11), we obtain the decay rate for the transiently chaotic region,

$$\bar{\alpha} = \sum_k \alpha_k, \quad (12a)$$

where

$$\alpha_k = f_Q(u_k) \Delta A_k \quad (12b)$$

and the sum is over all stable primary fixed points  $u_k$  in the region  $u_s < u < u_b$ .

The first entry in Table I gives the exponential decay rate  $\bar{\alpha}$  determined by numerical iteration of 100 random initial phase points at low velocities; the second entry gives the analytical result (12). The agreement is seen to be quite reasonable.

We have seen that all initial points are ultimately attracted to the stable fixed points of the map. The fraction  $\mu_k (= \alpha_k/\bar{\alpha})$  of initial phase points that ultimately stick to the various main-island fixed points (including their secondary fixed points) can also be found analytically with use of (12b). In Fig. 2, we plot the ratio  $R_k = \mu_k(\text{analytical})/\mu_k(\text{numerical})$  for all stable  $u_k$  for the cases in Table I. For  $M=30$ ,  $k=3, 4$ ; for  $M=100$ ,  $k=5-8$ ; for  $M=300$ ,  $k=9-16$ . We see that (12b) agrees well with the numerical results. Even better agreement is obtained by use of  $\gamma=3$  in (8), particularly for those islands that are close to the adiabatic barrier  $u_b$ . We expect a better estimate for  $\bar{D}$  in (8) to yield even closer agreement to the numerical results for  $\bar{\alpha}$  and  $\mu_k$ .

Several additional features observed numerically remain to be brought within the framework of the theory presented here. In several cases in Table I, a few of the hundred initial conditions were attracted to a primary resonance having period two. These resonances,  $u_{n+2} = u_n$ ,  $\psi_{n+2} = \psi_n \pmod{2\pi}$ , are located near  $u_k \approx 2M/k$ ,  $k$  odd, and are stable within some parts of region (2). We believe that the effect of these higher-period sinks can be treated analytically by considering the square, cube, etc., of the map (1).

For the case  $M=100$ , the stochasticity parameter for the  $k=8$  fixed point at  $\delta=0$  is  $K \approx 4.02$ . Thus this fixed point is linearly unstable, and a stable, bifur-

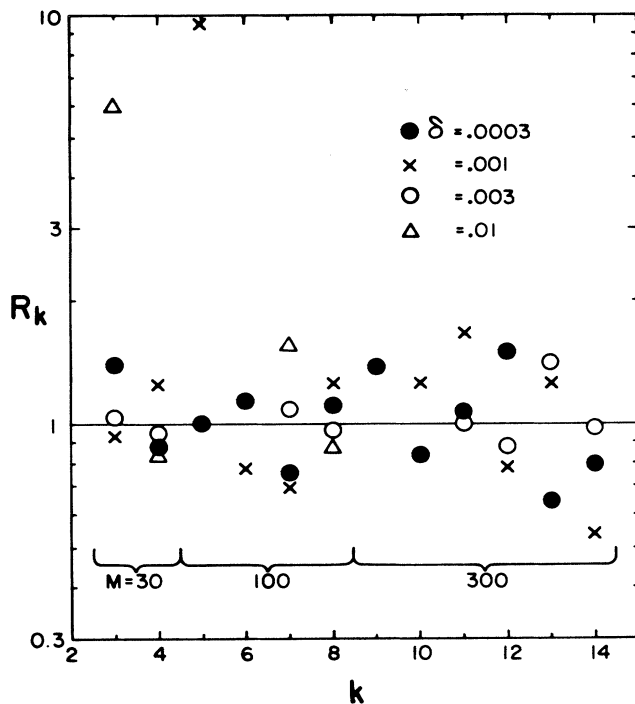


FIG. 2. The ratio  $R_k$  of the analytically to numerically determined fractions  $\mu_k$  of initial phase points attracted to the various island sinks, for all the cases given in Table I.

cated periodic orbit appears nearby.<sup>2</sup> However, a KAM barrier having area  $\bar{A}$  still surrounds this period-2 orbit. The size of  $\bar{A}$  depends delicately on  $\delta$ . Thus we determined  $\bar{A}$  by numerically iterating the map (5) with  $\delta$  set equal to zero in the first term on the right-hand side of (5a). In general, the areas of the stable period-2, -4, etc., islands are small.

Another numerical observation is that within each island surrounding a primary sink at  $u_k$ , there are a number of secondary sinks having periods greater than 1. For example, Fig. 1 shows a period-5 secondary sink surrounding the primary sink at  $u_3 = 10$ , and a period-3 secondary surrounding the primary sink at  $u_4 = 7.5$ . We determined in (12) only the total fraction of initial orbits eaten by an island, and not the distribution among the primary and secondary sinks within the island. We believe that the latter distribution might be determined by first transforming to obtain the separatrix mapping<sup>2,8</sup> associated with the primary resonance  $u_k$  and then applying the theory presented here to the separatrix mapping. The procedure for effecting this renormalization transformation from pri-

mary to secondary resonances is described in Ref. 1, Sects. 2.4 and 4.3. The technique may also be applicable to the special class of maps, studied by Feigenbaum, Kadanoff, and Shenker<sup>22</sup> and Ostlund *et al.*,<sup>23</sup> in which a single (attracting) invariant circle is retained when the map is dissipatively perturbed.

An expanded description of our technique and results is in preparation.<sup>24</sup> The support of the Office of Naval Research, Contract No. N00014-84-K0367, and the National Science Foundation, Grant No. ECS-8104561, is gratefully acknowledged.

<sup>1</sup>A. J. Lichtenberg and M. A. Lieberman, *Regular and Stochastic Motion* (Springer-Verlag, New York, 1982), Appendix A.

<sup>2</sup>Ref. 1, Chap. 3.

<sup>3</sup>R. H. G. Helleman, in *Fundamental Problems in Statistical Mechanics V*, edited by E. G. D. Cohen (North-Holland, Amsterdam, 1980), p. 165.

<sup>4</sup>R. Shaw, *Z. Naturforsch., Teil A* **36**, 80 (1981).

<sup>5</sup>E. Ott, *Rev. Mod. Phys.* **53**, 655 (1981).

<sup>6</sup>K. Y. Tsang and M. A. Lieberman, *Physica (Amsterdam)* **11D**, 147 (1984).

<sup>7</sup>K. Y. Tsang and M. A. Lieberman, *Phys. Lett.* **103A**, 175 (1984).

<sup>8</sup>B. V. Chirikov *Phys. Rep.* **52**, 263 (1979).

<sup>9</sup>G. M. Zaslavskii, *Phys. Lett.* **69A**, 145 (1978).

<sup>10</sup>E. Fermi, *Phys. Rev.* **75**, 1169 (1949).

<sup>11</sup>M. A. Lieberman and A. J. Lichtenberg, *Phys. Rev. A* **5**, 1852 (1972).

<sup>12</sup>G. M. Zaslavskii and B. V. Chirikov, *Dokl. Akad. Nauk SSSR* **159**, 306 (1964) [*Sov. Phys. Dokl.* **9**, 989 (1965)].

<sup>13</sup>A. Brahic, *Astron. Astrophys.* **12**, 98 (1971).

<sup>14</sup>A. J. Lichtenberg, M. A. Liebermann, and R. H. Cohen, *Physica (Amsterdam)* **1D**, 291 (1980).

<sup>15</sup>Ref. 1, pp. 436-442.

<sup>16</sup>Ref. 1, Sect. 5.4.

<sup>17</sup>Ref. 1, Sect. 4.1.

<sup>18</sup>A. B. Rechester, M. N. Rosenbluth, and R. B. White, *Phys. Rev. A* **23**, 2664 (1981).

<sup>19</sup>N. W. Murray, M. A. Lieberman, and A. J. Lichtenberg, *Phys. Rev. A* (to be published).

<sup>20</sup>A. J. Lichtenberg, *Nucl. Fusion* **24**, 1277 (1984).

<sup>21</sup>B. B. Chirikov and F. M. Izraelev, *Physica (Amsterdam)* **2D**, 30 (1984).

<sup>22</sup>M. J. Feigenbaum, L. P. Kadanoff, and S. J. Shenker, *Physica (Amsterdam)* **5D**, 370 (1982).

<sup>23</sup>S. Ostlund, D. Rand, J. Sethna, and E. Siggia, *Physica (Amsterdam)* **8D**, 303 (1983).

<sup>24</sup>K. Y. Tsang and M. A. Lieberman, to be published.